PROCEEDINGS B

royalsocietypublishing.org/rspb

Research

Cite this article: Poulin E, Kolmann MA, Stiassny MLJ, Cohen KE, Huie JM, Chabain JJ, Martinez CM. 2026 Stingray spine diversity reflects performance trade-offs linked to puncture and breakability. *Proc. R. Soc. B* **293**: 20260545.
https://doi.org/10.1098/rspb.2026.0545

Received: 7 March 2026
Accepted: 22 May 2026

Subject Category:
Morphology and biomechanics

Subject Areas:
biomechanics, evolution, ecology

Keywords:
defensive morphology, evolutionary ecology, functional morphology, micro-CT, Myliobatiformes, trade-offs, puncture mechanics

Author for correspondence:
Emily Poulin
e-mail: epoulin@uci.edu

Electronic supplementary material is available online at https://doi.org/10.6084/m9.figshare.c.8533457.

THE ROYAL SOCIETY PUBLISHING

Stingray spine diversity reflects performance trade-offs linked to puncture and breakability

Emily Poulin[1], Matthew A. Kolmann[2], Melanie L. J. Stiassny[3], Karly E. Cohen[4], Jonathan M. Huie[1], Jules J. Chabain[5] and Christopher M. Martinez[1]

[1]Department of Ecology and Evolutionary Biology, University of California Irvine, Irvine, CA 92697, USA
[2]Department of Biology, University of Louisville, Louisville, KY 40208, USA
[3]Department of Ichthyology, American Museum of Natural History, New York, NY 10024, USA
[4]Friday Harbor Laboratories, University of Washington, Seattle, WA 98250, USA
[5]Department of Evolution, Ecology, and Behavior, University of Illinois at Urbana-Champaign, Urbana, IL 61801, USA

EP, 0000-0001-7218-9752; MAK, 0000-0001-9748-2066; MLJS, 0000-0001-8220-4768; KEC, 0000-0001-6556-5414; JMH, 0000-0002-7925-7372; JJC, 0009-0008-2546-2187; CMM, 0000-0001-5930-4189

Stingrays (order Myliobatiformes) possess defensive spines that inflict intense pain through mechanical damage and envenomation. These spines exhibit striking variation among species, yet the functional underpinnings of their morphological diversity remain poorly understood. We analysed spine functional morphology across 30 species from five families to characterize variation along phylogenetic and ecological gradients. Spines ranged from slender, sharp-tipped forms with low-profile serrations to robust and wide-tipped with more prominently projecting serrations. By integrating morphological data with finite element modelling and puncture and removal tests, we uncovered biomechanical trade-offs shaping stingray spine evolution. At one extreme, slender, sharp-tipped spines puncture deeply but are prone to breakage, while robust spines resist fracture and anchor more effectively, though with reduced puncture performance. These contrasting morphologies likely represent divergent defensive strategies—spines that readily fracture maximize damage through breakage and retention in predator tissues, facilitating escape. Conversely, more durable spines may be reused across multiple defensive bouts. The latter are often in freshwater stingrays, potentially linked to habitat-specific features like refuge availability. Our findings suggest that trade-offs between puncture, anchoring and durability have been central to stingray spine evolution. Similar patterns across taxa suggest shared mechanical constraints shaping the evolution of biological weapons.

1. Introduction

Organisms have evolved an array of defensive structures to resist predation and, like all functional traits, they are subject to various constraints and trade-offs [1,2]. The effectiveness of a defensive structure is shaped by the physical forces it must withstand and the ecological contexts in which it operates [2,3]. Some defensive structures prioritize durability, like rigid exoskeletal shields or reinforced armour plates that absorb repeated impact forces and broadly distribute stress [4,5]. Other structures deter predators through the use of sharp projections or barbed surfaces, which inflict pain and hinder future attacks [6,7]. A common feature of defensive structures is their tendency to maximize one aspect of performance at the expense

of another [1,2]. Heavy armour often increases protection yet limits mobility [8,9], while sharp structures designed to inflict damage risk fracture or breakage upon impact [10,11]. Such trade-offs have evolutionary consequences that are expected to shape the diversity of defensive structures across lineages.

Although united by the mechanical demands of puncture, defensive spines serve diverse functions [2,3]. For example, some cactus spines puncture passively and anchor in tissue using microscopic barbs that snag on fibrous tissues and resist withdrawal [7]. Conversely, wasp stingers are comparatively robust to repeated use, facilitating the ease of removal rather than anchoring [12]. The ability to reuse versus sacrifice defensive structures may represent a central trade-off underlying spine evolution, as temporary reductions in defensive performance during regeneration are expected to increase predation risk [13]. Ecological factors and functional trade-offs are also expected to shape the diversity of spines across plants and animals.

Stingrays (order Myliobatiformes) comprise a diverse group of elasmobranch fishes occupying a wide range of marine habitats, but also occur within some freshwater systems [14]. They are generally united by the presence of prominent defensive spines positioned along their tails (electronic supplementary material, figure S1), though the structure has been lost in some lineages [15]. The spines are modified dermal denticles composed of an outer enamel-like layer and an inner mineralized dentine core [16]. Species range from having one to eight spines per individual, and when multiple spines are present, they are stacked in a similar location on the tail [17]. Spines range from 8 to >338 mm [18–21] and are shed and replaced annually to semi-annually [16,22]. When a stingray is threatened, its defensive spines are rapidly deployed against predators using a whip-like tail strike, which inflicts damage through puncture, laceration and envenomation [23,24]. Furthermore, spines are morphologically diverse across stingrays, in a manner suggesting evolved variability in defensive performance among species [18–21,25].

Whether a spine is withdrawn for reuse or fractures and remains embedded could be critical to a stingray's ability to continually defend itself. Spines of some marine stingrays have been found deeply embedded in the tissues of predators. Embedded spines have been documented in wedgefish (*Rhynchobatus*) jaws, cobia (*Rachycentron canadum*) skulls, and the skeletal tissue of bottlenose dolphins (*Tursiops truncatus*) and killer whales (*Orsinus orca*) [26–29]. Injuries associated with stingray spines can be severe and, though rare, have been fatal in humans and large predators like killer whales [24,29]. While embedded spines have been documented in marine predators, comparable observations are lacking for freshwater predators of stingrays, though it is unclear whether this is due to observational biases. Still, the types of predators encountered and availability of habitat structure differ between marine and freshwater systems [30,31], and are likely central to the nature of predator–prey interactions and to the evolutionary pressures for spine function. The extent to which diversity in spine morphology across stingrays contributes to variation in defensive behaviour and performance is not well understood. However, the implications are important, as spines optimized for reuse versus breakage could additionally influence venom delivery, escape success and the degree of damage inflicted towards predators.

In this study, we explore performance implications of stingray spine diversity, focusing on potential trade-offs shaping the evolution of this iconic defensive structure. Using a suite of functionally relevant traits, we assessed macroevolutionary patterns of stingray spine variation as a means of defining its major axis of diversity. Spine performance was assessed by computational modelling of structural stresses with finite element analysis (FEA) and experiments using three-dimensionally printed idealized physical models to test puncture and removal mechanics. We predicted that variation in spine and serration morphology would correspond to differences in puncture, removal and breakage performance. Specifically, we were interested in whether certain morphologies optimize puncture efficiency while others enhance durability and anchoring. While venom delivery is an important aspect of stingray defence, and certainly evolved alongside spine morphology, we focus on the functional and mechanical aspects of spine diversity that can be measured in a comparative framework from museum specimens. Based on our results, we discuss how selection shapes defensive traits within the bounds of mechanical constraints and phylogenetic conservatism. More broadly, we frame our work in the context of trade-offs in biological weaponry and explore the degree to which structural adaptations balance competing functional demands at a macroevolutionary scale.

2. Methods

(a) Specimen sampling and micro-computed tomography scanning

We used high -resolution micro-computed tomography (μCT) scans to compare spines across 30 marine and freshwater species of myliobatiform stingrays, based on 37 specimens from 10 of 37 genera and 5 of 11 families (electronic supplementary material, table S1, figure S2) [32,33]. The goal of our sampling scheme was to represent the range of spine morphologies across the order to assess its functional implications. We used 3D Slicer to digitally render, segment and isolate the spines for further analysis [34,35]. To reduce variation related to developmental stage, we excluded underdeveloped spines from our analyses as well as those that were newly emerging during regular replacement. For further details about scan settings and locations, see electronic supplementary material, Methods.

(b) Spine functional morphology traits

We measured a series of morphological traits expected to influence spine performance during defensive behaviours (figure 1) ([25]; see [18–21]). From a dorsal view, we measured the included angle (a measure of tip sharpness) in degrees using Image J [37], which affects how easily a spine's leading edge can puncture tissue [38]. We measured the serrated proportion of the spine's total length (length of serrated edge divided by total spine length, measured from tip to base in mm), serration length

(length of an individual serration at spine midpoint divided by total spine length, both in mm) and serration angle (projection relative to the primary spine axis, in degrees). These serration properties correspond to the spine's potential to damage and interact with tissue during both puncture and withdrawal [25]. Spine aspect ratio (spine length divided by shaft width at 50% of spine length, both in mm) influences the spine's overall profile, potentially affecting its ability to puncture and maintain structural integrity during defensive interactions [11,39]. In 3D Slicer, the surface area to volume ratio (SA:Vol) was measured in the *Segment Statistics* module. SA:Vol integrates size and shape effects, potentially influencing puncture efficiency [38,40]. Using the *SegmentGeometry* module [41], we measured the maximum second moment of area around the minor principal axis (I_{minor}, in mm^4) at the midpoint of the spine and corrected for cross-sectional size using material normalization (MatNorm).

We used phylogenetic comparative methods to explore spine functional diversity across stingray species and to assess performance consequences. Analyses were conducted using a summary tree constructed with TreeAnnotator in BEAST (v.10.5.0) [42], estimated from a distribution of 10 000 time-calibrated trees from Stein *et al*. [36]. Analyses were also done on 500 randomly sampled trees from the original 10 000-tree distribution to address the potential role of phylogenetic uncertainty on our results. The full tree from Stein *et al.* [36] was inferred based on a subset of taxa with molecular data, to which additional taxa were imputed based on taxonomy. To examine whether imputed species impacted our results and their interpretations, we also ran analyses using a tree containing only the taxa for which molecular data were available (n = 22 species).

All statistical analyses were conducted in R (v.4.4.1) [43]. For species in which multiple individuals were sampled, average trait values were calculated. Traits based on ratios were first log-transformed due to expected non-normality of ratio data (proportion serrated, serration length, surface area to volume ratio and spine aspect ratio). All traits were tested for normality using the Shapiro–Wilk test (*shapiro.test*). We used a principal component analysis (PCA) to visualize spine functional diversity and characterize the primary axes of variation. The PCA was performed on the correlation matrix (i.e. scale = TRUE) using the *gm.prcomp* function from the geomorph package (v.4.0.10) [44,45].

Prior to multivariate statistical analyses, we scaled and centred trait data with the scale function in R to ensure the variables were commensurate. To test for differences in multivariate means of spine morphometric traits based on habitats (i.e. marine versus freshwater), we conducted a phylogenetic multivariate analysis of variance (MANOVA) using the *procD.pgls* function from geomorph (10 000 iterations). We also examined the relationship between habitat and each trait individually using phylogenetic ANOVAs (*phylANOVA*) in phytools (v.2.4-4) [46] based on 10 000 simulations. Additionally, we compared variance among the morphometric traits collectively, and individually, across habitats using the *morphol.disparity* function in geomorph (10 000 iterations).

(c) Spine performance (computational models)

We assessed the performance implications of stingray spine morphology with two approaches: a computational model of stress in response to applied force (FEA) and physical model testing. FEA allows for evaluation of spine performance under modelled scenarios to compare mechanical stress responses across morphologically diverse spines, using three-dimensional geometries derived from micro-CT scans. To evaluate how stingray spines respond to stress and bending, we simulated two loading scenarios in FEBio Studio (electronic supplementary material, figure S3) [47]. For the first scenario, representing dorsoventral cantilever bending, we fixed the base of the spine in all degrees of freedom and applied a point force at the distal tip in the dorsoventral direction. In this scenario, the dorsal surface experiences tension while the ventral surface is under compression. The second scenario represented lateral cantilever bending. We again fixed the base of the spine in all degrees of freedom and applied a point force at the distal tip perpendicular to the dorsoventral plane. This produced lateral bending, with the side of the spine in the direction of loading in compression and the opposite side in tension. These scenarios were intended to approximate loading during puncture and removal, where the spine base is constrained by attachment to the tail and the embedded tip experiences loading that induces bending. The applied load was scaled by volume across all models (0.5 N cm^{-3}) to ensure comparability across spines [48]. In both cases, we used the volume-averaged mean first principal stress across the model, which reduces sensitivity to localized stress concentrations relative to maximum stress values [49]. Further details regarding scan preparation and model specification can be found in the electronic supplementary material, methods.

We examined the relationship between habitat and average first principal stress, using phylogenetic ANOVAs (*phylANOVA*) in phytools based on 10 000 simulations. Phylogenetic generalized least squares (PGLS) regressions of stress measured from FEA scenarios on individual morphological traits were used to examine covariation while accounting for phylogenetic non-independence. Separate tests were conducted for each FEA scenario (i.e. dorsoventral and lateral bending), analysing the relationships between average stress and: (i) each axis of spine diversity (PC scores), and (ii) each functional morphology trait, individually. For each PGLS regression, a Brownian motion correlation matrix was applied, and the analysis was performed using the *gls* function from the nlme package [50]. Model fit for statistically significant PGLS models was summarized using a likelihood-based R^2 [51].

(d) Spine performance (physical models)

To further explore the performance consequences of spine diversity, we generated a series of idealized physical models that reflect key features of morphological variation linked to puncture and removal ability. These models were designed to capture variation along the primary axis of morphological diversity (PC1), emphasizing traits that loaded strongly on this axis. As a result, additional variation in traits not strongly correlated to PC1 are not represented in these models. The goal of these

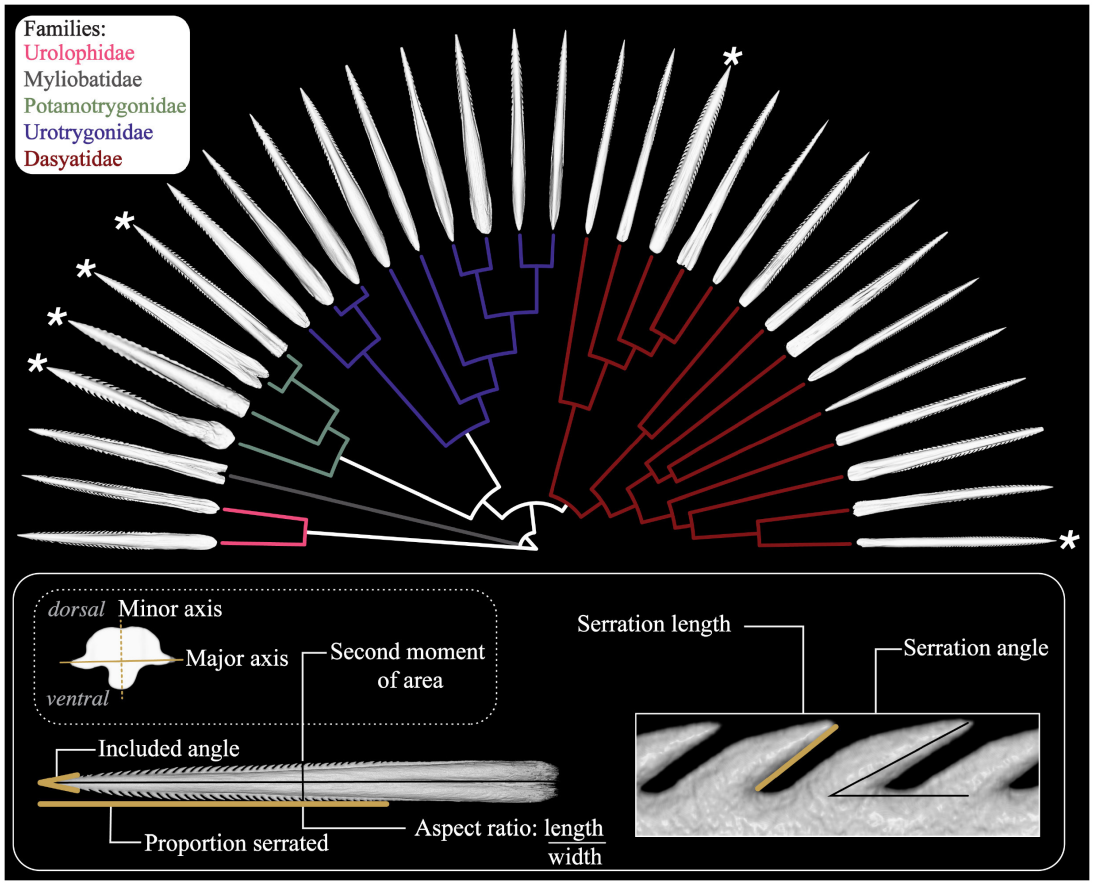

Figure 1. Sampling of spine morphologies and functional morphology traits. Top, phylogenetic relationships of stingray species sampled in this study, colour-coded by family (tree: [36]). A micro-CT scan of a spine for each study species is included at the tips of the tree (spines are scaled to uniform length to emphasize shape variation). Asterisks indicate freshwater taxa. Bottom, spine morphological traits, shown on a micro-CT scan from the freshwater stingray, *Potamotrygon orbignyi*. Included angle measures tip sharpness. Proportion serrated represents length of serrated edge relative to spine total length. Aspect ratio is the spine length divided by width at 50% of the spine's length, describing overall robustness. Second moment of area describes resistance to lateral bending based on cross-sectional shape, measured at the spine midpoint around the minor principal axis. Serration length is measured at the spine midpoint and is expressed relative to spine length. Serration angle reflects degree of projection relative to the primary spine axis.

models was to isolate the relative effects of this morphological variation on performance, rather than to reproduce the actual performance of real spines. For this, we used spines' included angle, angle of serration, serration length and the proportion serrated. Shaft morphology was held constant across models while tip and serration traits were modulated. For each trait, we estimated their hypothetical values at five evenly sampled points along the primary axis of spine variation, PC1, from a PCA of spine functional traits. Five models were constructed, and each was given the combination of estimated spine trait values for their location along PC1 (electronic supplementary material, figure S4, Methods). Models were constructed in Autodesk TinkerCad [52], smoothed in Blender and three-dimensionally printed using a Formlabs 3+printer with Clear V5 photopolymer resin.

To test the puncturing ability of spine models, we built a drop-tester to pierce an analogue for vertebrate flesh at biologically relevant strike speeds. Because the response of biological tissues during puncture varies with impact speed [53], we quantified puncture and removal performance under dynamic, high-velocity conditions. Complimentary quasi-static trials were used to measure peak puncture and removal force at a displacement rate of 100 mm min^{-1} [53]. The quasi-static tests are sufficiently slow that inertial effects during puncture and removal are expected to be small or negligible. The dynamic and quasi-static experiments differed in loading rate, equipment, target material, and the extent of spine engagement during puncture and removal. Therefore, values are not directly comparable between tests. Instead, each approach was used to assess relative performance trends among models. Full details of the quasi-static methods and results are reported in the electronic supplementary material.

All tests of puncture and removal were oriented perpendicular to the target, consistent with observations that during vertical defensive strikes the spine is held nearly perpendicular to the threat at impact [23]. Our objective for each set of puncture and removal trials was to use a consistent target material to facilitate comparisons of relative performance values across spine models. We used Ecoflex silicone, which is isotropic, homogeneous and has a shore hardness within the range observed for vertebrate (human) flesh [54]. Ecoflex 00-30 target cubes were used for all trials except dynamic puncture. For the latter, Ecoflex 00-20 was used to achieve measurable puncture depths within the sensitivity range of our drop tester. Target cubes used for dynamic puncture measured 6 × 6 × 5 cm. In dynamic puncture tests, spines were dropped from a height of 53 cm and reach a velocity of 323 cm s^{-1} at the time of puncture, which is of comparable magnitude to experimental observations (i.e. 213 cm s^{-1} average strike speed in [23]).

To measure spine removal force, we constructed a ballistic pendulum apparatus that dislodges a spine embedded in silicone at high speeds (electronic supplementary material, figure S5) [53]. The pendulum travelled up to 352 cm s^{-1}. Each spine model was embedded point-first by manually pushing it through a silicone target cube until the cuboid base at the shaft's end was touching the outer surface of the target. The removal force needed to withdraw the spine from the silicone block was calculated by determining the change in gravitational potential energy between the initial and final stages of the pendulum swing (see calculation details in the electronic supplementary material). Spine models were withdrawn from silicone target cubes measuring 5 × 5 × 3 cm with a Shore hardness score of 00-30.

All performance metrics were tested for normality (*shapiro.test*), and a one-way ANOVA was used to test for differences in mean puncture distance and removal force between physical models sampled along the primary axis of morphological diversity with the *aov* function in R. *Post hoc* pairwise comparisons between models were conducted using Tukey's honestly significant difference with the *TukeyHSD* function.

3. Results

(a) Spine functional morphology

After appropriate transformations, when applicable, none of the morphological traits or performance metrics considered in this study deviated significantly from normality based on Shapiro–Wilk tests (electronic supplementary material, table S2). A PCA on all morphological traits revealed major axes of stingray spine diversity (figure 2). The primary axis, PC1, contained 39.1% of total spine variation and reflected differences in included angle, serration angle and aspect ratio. Along this axis, dasyatid and urotrygonid stingrays span much of the range from low to intermediate values, with the lower extreme associated with thin (high aspect ratio) spines with more pointed tips and lower profile serrations. Freshwater potamotrygonid stingrays occupied the upper limits of PC1 with comparatively robust and dull-tipped spines with more laterally projecting serrations. The urolophids form a small central cluster that did not overlap with other families. PC2 contained 16.5% of total variation and primarily reflected variation in the second moment of area at the spine's midpoint and proportion serrated. Along this axis, lower extremes were associated with wide spines (high second moment of area) with a small proportion serrated. Along PC2, divergence was observed between urotrygonid (lower range) and dasyatid (upper range) stingrays. Additionally, the potamotrygonids spanned nearly the entire range of PC2. Families occupied mostly non-overlapping regions within the morphospace defined by PCs 1 and 2.

Statistical results for spine morphology were largely consistent across analyses using a summary tree, a distribution of 500 trees and a molecular-only tree excluding imputed taxa, so we report only the former in the main text but make note of any exceptions and include results for all three approaches in relevant supplemental tables. In four instances, analyses based on species limited to the molecular-only tree were significant, but results based on a summary tree with higher taxon sampling were not. Here, we took a conservative approach, favouring the non-significant results based on the full dataset, and make conclusions and interpretations accordingly. Consequently, we did not consistently recover any significant differences in means of functional morphology traits by habitat, either in a multivariate context or individually ($p > 0.05$ in all cases; electronic supplementary material, table S3; figure S6), though one likely factor is limited phylogenetic replication in freshwater rays which are dominated, in large part, by a single family (Potamotrygonidae). Similarly, we found no significant differences in trait variance across habitats ($p > 0.05$ in all cases; electronic supplementary material, table S4).

(b) Spine performance (computational models)

Stresses resulting from applied forces in FEA models showed relationships with key morphological traits (figure 3; electronic supplementary material, table S5). For the dorsoventral bending model, average first principal stress had a strong negative relationship with PC1 (PGLS; $p = 8.33 \times 10^{-6}$, $R^2 = 0.51$). This model also showed a positive relationship with spine aspect ratio (PGLS; $p = 8.68 \times 10^{-9}$, $R^2 = 0.70$). Simulated average stress varied substantially across species, with a 2.6-fold difference between the lowest- and highest-stress spines. The dorsoventral model also had a negative relationship with the serration angle (PGLS; $p = 8.76 \times 10^{-4}$, $R^2 = 0.33$) and proportion serrated (PGLS; $p = 0.025$, $R^2 = 0.17$). Additionally, the lateral bending model showed similar trends, with a negative relationship between stress and PC1 (PGLS; $p = 7.13 \times 10^{-7}$, $R^2 = 0.59$), and a positive relationship with aspect ratio (PGLS; $p = 4.49 \times 10^{-11}$, $R^2 = 0.79$). Here, average stress differs by up to 2.1-fold across species. The lateral bending model also displayed negative relationships with the included angle (PGLS; $p = 5.02 \times 10^{-10}$, $R^2 = 0.25$) and serration angle (PGLS; $p = 0.021$, $R^2 = 0.18$). Additional comparisons of modelled stresses with other morphological traits or PC axes 2 through 7 mostly showed mixed or no relationship (electronic supplementary material, tables S5, S6).

(c) Spine performance (physical models)

Morphological variation among physical spine models impacted both puncture depth and removal resistance (figure 4). Five models, labelled 1 to 5, represented morphological variation along PC1, from minimum (model 1) to maximum values (model 5; yellow dots indicate sampling locations in figure 4). Model 1 exhibited the sharpest tip (lowest included angle), the most recurved serrations (lowest serration angle), the smallest proportion of serrated length and the shortest serrations (electronic supplementary material, table S7). Subsequent models each displayed increasing values for these traits.

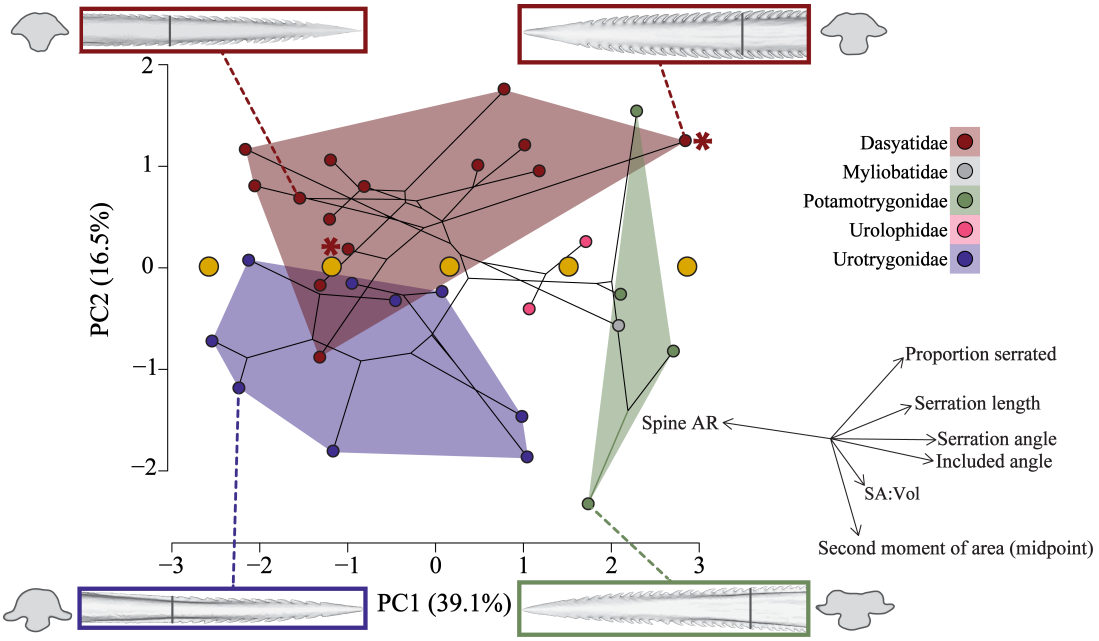

Figure 2. Principal component analysis (PCA) of seven morphological traits measured from spines of 30 stingray species (colour-coded by family). Vectors showing trait loadings on the principal axes are shown to the right. Red asterisks indicate locations of *Fontitrygon garouaensis* (left) and *Fluvitrygon signifer* (right), two independent transitions to a freshwater lifestyle outside of the fully freshwater family, Potamotrygonidae. Cropped images of spines from *Hypanus sabinus* (upper left), *Fluvitrygon signifer* (upper right), *Urotrygon chilensis* (lower left) and *Potamotrygon motoro* (lower right) represent morphological variation across the plotted axes. Vertical grey lines denote the spine midpoints, and silhouettes show the cross-sectional shape at these locations. Yellow dots indicate five locations along PC1 where trait values were estimated for the creation of physical models.

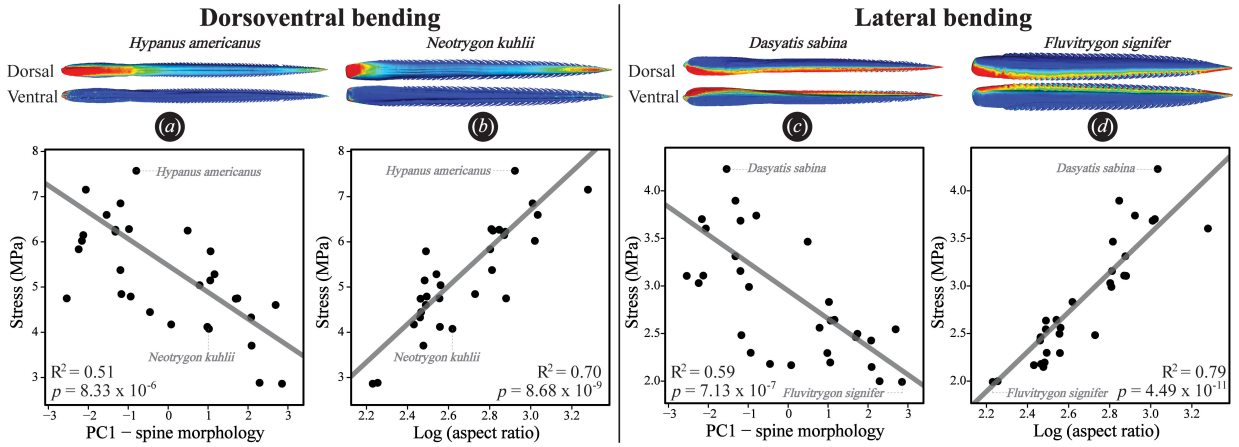

Figure 3. Relationships between species-averaged first principal stresses from FEA simulations and spine morphological traits. (*a* and *b*) Stresses modelled after a dorsoventral bending test plotted against the primary axis of spine morphological variation (PC1 values from figure 2) and spine aspect ratio. (*c* and *d*) Stresses generated by lateral bending plotted against PC1 values and spine aspect ratio. *P*-values from PGLS regressions and likelihood-based R^2 values are indicated on each panel, with stress increasing in high-aspect-ratio spines and showing negative associations with PC1. Locations of *Hypanus americanus*, *Neotrygon kuhlii*, *Dasyatis sabina* and *Fluvitrygon signifer* are indicated, representing examples of relatively high and low average stress values across loading scenarios.

In dynamic puncture tests, models showed significant overall differences in their puncture depth (ANOVA; $F = 14.02$, $p = 4.69 \times 10^{-7}$). Dynamic spine removal tests also showed significant differences among models in the average force required to extract spines from a flesh analogue (ANOVA; $F = 9.61$, $p = 5.77 \times 10^{-5}$). Pairwise results across models are included in electronic supplementary material, tables S8, S9. Collectively, dynamic performance tests revealed a consistent directional pattern in which models that punctured more deeply required lower average forces for removal, while models with shallower puncture depths required higher forces. Although quasi-static tests quantified puncture and removal performance using peak force rather than puncture depth or average force, they showed a broadly similar ordering among models and with consistent performance implications (electronic supplementary material, tables S10, S11; figures S7, S8).

4. Discussion

Across the tree of life, defensive structures have repeatedly evolved under competing ecological and functional pressures [1,2]. Stingray spines are critical defensive structures [23] that display broad morphological variation at a macroevolutionary scale.

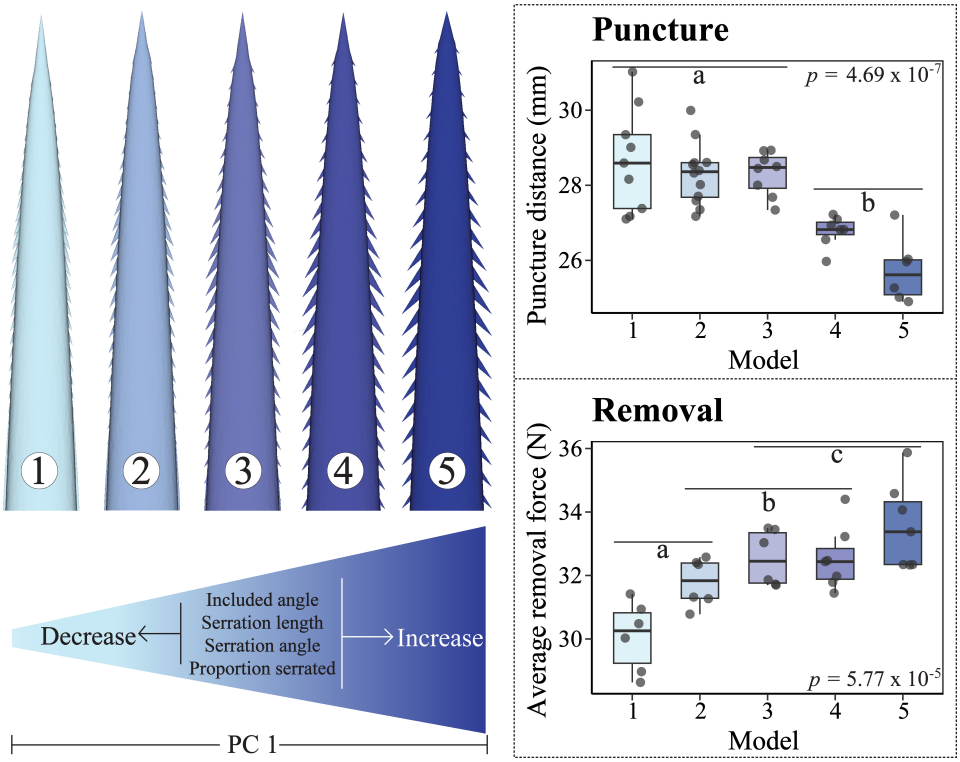

Figure 4. Dynamic puncture and removal performance of physical spine models at biologically relevant velocities. Models (left) represent trait combinations along the primary axis of spine diversity (PC1 from figure 2). Puncture depth was measured after spines were dropped vertically along a weighted track from a fixed height. Average removal force was measured by embedding spines to their full working length (92.2 mm) and then rapidly withdrawing them using a weighted pendulum. (Right) Top panel: boxplot showing reduced puncture distance for models representing higher PC1 scores. Bottom panel: boxplot showing increased average removal force associated with models at higher PC1 scores. *P*-values from overall ANOVAs are indicated on figure panels. Additionally, results from pairwise comparisons are shown, where models that do not share a lowercase letter in common are significantly different from each other ($p < 0.05$).

Our analyses reveal that their diversity is primarily characterized as a continuum reflecting overall robustness, tip sharpness and the projection of lateral serrations (PC1 in figure 2). These traits represent the features of spines that have experienced the greatest degree of diversification among major stingray lineages. Given the vital role that spines play in stingray survival, the observed patterns are thought to reflect divergent demands on spine function and defensive performance that have arisen during the group's evolutionary history. This is consistent with observations that morphological evolution of spines in other animal systems is attributed to differences in use and predation risk [2,55,56]. Our results suggest that stingray spines similarly evolved along axes that carry important performance implications, and that key trade-offs in puncture, anchoring and durability likely underlie differences in defensive interactions.

(a) Breakability underlies a major axis of spine diversity

Structural failure is a feature of defensive spines, enabling strategic breakability [57]. While puncture performance is important for inflicting mechanical damage and effective venom delivery, the ability to fracture can be equally critical by creating opportunities for an organism to escape predation attempts. In a manner analogous to tail autotomy in lizards [13], spine breakage allows an organism to shed part of its body to distract a predator and escape. Large marine predators of stingrays have been found with broken spines embedded in their jaws [26,58], indicating breakage as a regular occurrence in predatory interactions for some species. We found that stingrays with high aspect ratio spines experience greater average stress, and therefore a higher likelihood of breakage in response to simulated forces compared with those with lower aspect ratios (figure 3). Furthermore, this gradient of breakability was strongly aligned with the primary axis of spine morphological diversity, suggesting that variation in fracture potential has been a key feature of stingray spine evolution.

Despite the negative connotation that breakage evokes, the structural fragility of high aspect ratio spines may enhance predator deterrence [59]. Our findings suggest that gracile, fracture-prone spines appear to be optimized for deep puncture, while their tendency to break may increase the likelihood of being retained in predator tissues. Embedded spines can trigger inflammation, pain, infection and may prolong venom exposure, resulting in localized and lasting tissue damage [24,60,61]. While evidence of spine breakage and anchoring in predators exists, stingrays have evolved a range of morphologies suggestive of variation in the potential for structural failure. The most robust spines encountered in this study had low aspect ratios and appear to represent an alternative defensive strategy that emphasizes spine durability. These sturdy spines exhibited significantly lower average stress in response to simulated forces (figure 3), suggesting they are less likely to fracture during use. This observation parallels patterns observed in red lionfish (*Pterois volitans*), where shorter and stiffer spines are more resistant to damage during defensive interactions than more flexible spines [62]. Unlike slender spines, more durable structures may be retained and reused across multiple encounters with predators, preserving the stingray's defensive capacity throughout

the replacement cycle [16]. Spines with greater structural durability could be selected for in environments where maintaining a persistent defence provides continued protection during repeated predator encounters [63].

(b) Spine serrations dictate puncture and anchoring performance

Lateral serrations are ubiquitous features ornamenting stingray spines but they vary substantially across species in their shape, size, orientation and the proportion of the spine they cover (figures 1 and 2). While these structures are commonly associated with resisting removal from predator tissues, our findings suggest they also impact puncture. Using physical models, we found that variation in spine morphology along the primary axis of diversity reflects a trade-off between puncture and removal (figure 4). At one extreme, spines with sharp tips and short, recurved serrations achieved deeper puncture and had low withdrawal resistance. At the opposite end of the spectrum, spines with longer, more laterally oriented serrations and wider included angles punctured shallowly but resisted removal more effectively. These patterns suggest that the diversification of stingray spine morphologies has been heavily influenced by the competing functional demands of puncture and removal.

The effects of spine serrations on puncture and removal performance can be explained by considering the interactions of these structures with predator tissues during defensive strikes. More laterally projecting serrations are better positioned to engage surrounding tissue fibres, anchoring the spine and increasing withdrawal resistance [6,7,12]. Longer serrations and those that cover a higher proportion of the spine's length (such as *Fluvitrygon signifer*, see figure 2) enhance this anchoring effect by increasing contact with surrounding tissues [6,7]. While larger and more laterally projected serrations may increase the anchoring ability of spines, these same features increase the spine's aspect ratio and decrease puncture depth (figure 4). Alternatively, spines with acutely angled serrations, paired with narrow included angles that concentrate force at the leading edge (see *Urotrygon chilensis*, figure 2), are expected to enhance puncture depth [6,38], but may be less effective at anchoring into surrounding tissues upon withdrawal if serrations do not effectively engage tissue fibres [12]. This geometry likely enhances puncture depth while minimizing resistance to removal.

Anchoring structures, like the serrations of stingray spines, have evolved in many organisms and serve important functions for both puncture and removal. Some cactus spines feature laterally projecting barbs that engage with tissues during withdrawal, which reduce puncture force but also increase resistance to removal [7]. Porcupine (family Erethizontidae) quills similarly possess recurved microscopic barbs that concentrate stress to reduce puncture force and anchor into tissue, increasing removal force [6]. Unlike these barbs, the serrations on stingray spines are rigid and do not change orientation during removal [25], and are substantially larger in scale. Our models indicated that more recurved serrations increased puncture depth while decreasing anchoring performance, suggesting that although both systems use recurved serration geometries to concentrate force, their functions could be scale and orientation dependent. The varied performance implications of serrations across species underscores how differences in size and combinations of serration attributes may reflect adaptive responses to varying threat landscapes.

(c) Performance trade-offs have left their mark on stingray spine evolution

Stingray spines exhibit clear trade-offs between puncture efficiency, anchoring ability and structural durability. Our work suggests starkly divergent performance strategies at the extremes of stingray spine diversity. Some species defend themselves using deep penetrating spines built to fracture and embed in prey (such as *Hypanus sabinus*, see figure 2), while others rely on robust and reusable spines that resist breakage and anchor more effectively (see *Potamotrygon motoro*, figure 2), but most contain spine traits that confer intermediate performance with respect to these attributes.

The patterns observed in stingrays are consistent with trade-offs found in defensive systems across animal diversity. The sea urchin *Diadema setosum* has long, hollow spines with barbs [64] that function as sacrificial defences, breaking off to protect the body [57]. Some urchin spines can easily fracture under stress and embed in would-be predators [59], potentially deterring further attack. On the other hand, the urchin *Lytechinus variegatus* has shorter, robust spines with solid internal architecture [65], which may reflect optimization for durability and may act more like armour than a puncturing weapon. In insects of the order Hymenoptera, honeybee stings are single-use defences that remain embedded in their target following puncture, while paper wasp stings require more force to puncture, but can be withdrawn and used repeatedly [12]. Finally, an extreme shift towards durability is seen in the hedgehog, *Erinaceus europaeus*, whose short, robust spines have evolved to act as shock absorbers during impact, such as during a fall [66]. The microstructure of these spines is specialized for storing elastic strain energy via controlled buckling, allowing for repeated use [66]. These examples highlight the many ways in which trade-offs between puncture and reusability have manifested, suggesting broader constraints on the design of defensive spines; high-aspect-ratio forms puncture deeply but risk structural failure, while robust morphologies sacrifice puncture efficiency for durability and repeated use. More broadly, our results reinforce how functional trade-offs between puncture, removal and durability collectively shape the diversification of defensive traits across diverse taxa.

(d) The influence of ecological factors on defensive spines

An intriguing outcome of this study is the observation that the spines of many freshwater stingrays fall out at morphological and functional extremes. Freshwater species, specifically in the family Potamotrygonidae, have robust spines with low-aspect ratios and laterally oriented serrations (figure 2). Taken together, the performance attributes of freshwater rays are puzzling from a defensive perspective: their spines require greater puncture force and are harder to dislodge, yet they are also resistant

to breakage—a combination that is not immediately intuitive (figures 3 and 4). One possibility that is consistent with our observed performance outcomes is that these spines have evolved as tools for scraping or slashing, rather than puncturing deeply. Hughes *et al*. [23] documented that the marine stingray *Urobatis jamaicensis* can deliver horizontal tail sweeps in addition to vertical strikes. This mode of behavioural modulation observed within a species may also be reflected among species, with some stingrays evolving specialized traits favouring horizontal (slashing) strikes over vertical (puncturing) strikes. While corroboration is needed, another observation in support of this hypothesis is that potamotrygonid rays possess venom glands that are more widely distributed along the spine and show higher venom toxicity compared with studied marine taxa [67,68]. This feature may reduce reliance on deep puncture, as effective envenomation could take place with a comparatively shallow stab or slash [69], and may help preserve the barb for future reuse.

Extreme morphological and performance traits observed in freshwater stingray spines may reflect the unique ecological and physiological pressures that these species face. Riverine habitats are structurally complex, with regions of submerged vegetation, topographic heterogeneity and dynamic floodplain microhabitats [31,70]. These features are likely to provide stingrays with greater opportunities to seek refuge and avoid defensive interactions, which could shape selective pressures experienced in freshwater habitats. In such areas, delivering a shallow injury with a robust, reusable spine could be more advantageous than puncturing deeply and risking spine breakage, as a stingray could escape into refugia following a defensive interaction. This strategy may be especially important for juveniles, as venom potency in freshwater stingrays declines with age and size, suggesting that smaller, more vulnerable individuals face greater need for potent venom [71]. In marine habitats, many stingrays inhabit open sand flats or pelagic environments where structural refuge is limited [72–74], potentially increasing selective pressure for spines that inflict deeper, more damaging wounds to predators.

Threats to stingrays are further distinguished between freshwater and marine systems by the different suites of predators occurring in each. In marine habitats, sharks are the primary and most prevalent predators of marine rays, and some species, such as hammerheads (*Sphyrna* spp.), are morphologically specialized to hunt them [30,75]. Additionally, marine cetaceans [29] and large predatory fishes prey on stingrays [26,30], as does the occasional crocodilian [76]. Lastly, there are a handful of observations of wading birds preying on juvenile rays in shallow marine habitats [77]. In freshwaters, river dolphins (*Inia geoffrensis*) [78] and large catfishes (order Siluriformes) [79] are apex predators that may represent potential sources of predation risk to potamotrygonids, while caimans are allegedly uncommon predators of freshwater rays [80]. However, vast areas of the Amazon basin where most freshwater rays are found remain poorly sampled, and the predator–prey dynamics in these systems are not well understood [31]. Additionally, variation in the tissue properties of major predators may influence the mechanical performance of defensive spines [81]. Improved knowledge of these interactions will be essential to understanding the evolutionary pressures shaping freshwater stingray defences.

The idea that habitat structure and predator exposure may influence the evolution of defensive morphologies across diverse vertebrate lineages is supported by the literature (e.g. [8,82]). Mammals in open environments lacking habitat cover are more likely to evolve structurally reinforced antipredator traits, such as spines or armour, due to increased exposure and reduced access to refugia [82]. Similarly, armoured cordyline lizards that live in exposed environments develop more robust body armour compared with species that live in protected habitats [8]. In both cases, habitat cover was a stronger predictor of defensive morphology than predation risk, suggesting that environmental exposure is central to shaping the evolution of defensive structures.

It is worth pointing out that although most freshwater stingrays belong to a single family, Potamotrygonidae, our dataset also includes two instances of independent freshwater colonizations within the predominantly marine family Dasyatidae, *Fluvitrygon signifer* and *Fontitrygon garouaensis*. Interestingly, *F. signifer* exhibits robust low-aspect-ratio spines with laterally oriented serrations, similar to those of potamotrygonid rays (figure 2). By contrast, *F. garouaensis* retains traits typical of its closest relatives, marine dasyatids. These findings suggest that independent freshwater transitions can carry mixed implications for spine morphology and trait evolution after habitat transitions [83]. Future work examining whether the two described marine potamotrygonid species (genus *Styracura*) depart from the freshwater clade would provide valuable insight into habitat-associated divergence within Potamotrygonidae. Additionally, *Myliobatis californica* overlaps with the potamotrygonid clade in morphospace, suggesting potential shared constraints on spine morphology between freshwater and pelagic taxa. Still, we caution that additional taxon sampling is necessary to determine whether these patterns reflect broader family-level trends.

(e) The role of venom in stingray defence

While this study focused on the structural and mechanical aspects of stingray spines, venom delivery is central to the effectiveness of their defensive interactions. Venom is delivered when the integumentary sheath covering the spine ruptures during puncture, allowing venomous tissue and secretions to be sloughed off directly into the wound [84]. This combination of mechanical injury and envenomation can cause intense pain and, in some cases, tissue necrosis and secondary infection [65]. The link between spine structural diversity and the effectiveness of venom delivery remains unclear. Traits that affect spine performance during puncture, anchoring, breakage and withdrawal could each influence venom transmission during an interaction with a predator, though further work is needed to test these predictions.

5. Conclusion

Stingray spines offer a compelling system to examine how defensive structures evolve under trade-offs shaped by biomechanical constraints and ecological pressures. By integrating morphological data, FEA and physical model testing, we identified the primary axes of functional variation in stingray spine morphology and its performance consequences. Stingray spines span a functional spectrum, with some morphologies optimized for deep puncture and breakage, while others for withdrawal and reuse. Spine performance is simultaneously shaped by the balance between puncture efficiency and removal resistance. The trade-offs observed in stingray spines reflect functional constraints that are echoed in the defensive phenotypes that have evolved at broader scales. The diversity of stingray spines reflects fundamental mechanical trade-offs shaped by ecological pressures, and this system contributes to our understanding of how functional constraints influence the evolution of defensive structures.

Ethics. This study used preserved museum specimens from existing collections and did not involve live animals, human subjects or fieldwork. Therefore, no ethical approval or collection permits were required. Specimen information is provided in the electronic supplementary material.

Data accessibility. The code scripts and data used for this study can be found on Dryad [85]. All three-dimensional data have been uploaded to MorphoSource (see Figshare [86]).

Supplementary material is available online [87].

Declaration of AI use. We have not used AI-assisted technologies in creating this article.

Authors' contributions. E.P.: conceptualization, data curation, formal analysis, funding acquisition, investigation, methodology, visualization, writing—original draft; M.K.: conceptualization, resources, writing—review and editing; M.S.: resources, writing—review and editing; K.C.: conceptualization, writing—review and editing; J.M.H.: investigation, writing—review and editing; J.C.: resources, writing—review and editing; C.M.M.: conceptualization, formal analysis, funding acquisition, investigation, methodology, project administration, resources, supervision, writing—review and editing.

All authors gave final approval for publication and agreed to be held accountable for the work performed therein.

Conflict of interest declaration. We declare we have no competing interests.

Funding. No funding has been received for this article.

Acknowledgements. Many people were instrumental in the collection of CT scan data for this paper, including Bill Ludt and Todd Clardy at the LACM, Jonathan Pfliger and Marta Bellato at the MNHN, Morgan Hill Chase and Department of Ichthyology collection staff at the AMNH, Kevin Conway and Heather Prestridge at TCWC, Mark Sabaj and Kyle Luckenbill at ANSP, Dave Catania and Jon Fong at CAS, and Rob Robins at FLMNH. We are grateful to Virginia Grace Enoch for help with segmenting spines and taking morphometric measurements. Darby Finnegan, Ben Nicholas and Justin Ng aided in the collection of pilot micro-CT data used in this project. We thank Matt McHenry and Monica Daley for helpful discussions at various stages of this research. Additionally, Mark Walter and Derek Irwin at UCI were helpful in providing assistance with force measurements. We thank Joyce Keyak, Cassandra Donatelli and Adam Summers for valuable discussions and research assistance during early stages of this project.

References

1. Cohen KE, Donatelli CM, Schulz AK, Teeple JB, Stankowich T, Paig-Tran EWM. 2025 Biological armors—evolution, materials, and bioinspiration. *Integr. Comp. Biol*. **65**, 1649–1666. (doi:10.1093/icb/icaf074)
2. Crofts SB, Stankowich T. 2021 Stabbing spines: a review of the biomechanics and evolution of defensive spines. *Integr. Comp. Biol*. **61**, 655–667. (doi:10.1093/icb/icab099)
3. Anderson PSL, Crofts SB, Kim JT, Chamorro LP. 2019 Taking a stab at quantifying the energetics of biological puncture. *Integr. Comp. Biol*. **59**, 1586–1596. (doi:10.1093/icb/icz078)
4. Woodruff EC, Huie JM, Summers AP, Cohen KE. 2022 Pacific spiny lumpsucker armor—development, damage, and defense in the intertidal. *J. Morphol*. **283**, 164–173. (doi:10.1002/jmor.21435)
5. Yadav R, Naebe M, Wang X, Kandasubramanian B. 2016 Body armour materials: from steel to contemporary biomimetic systems. *RSC Adv*. **6**, 115145–115174. (doi:10.1039/c6ra24016j)
6. Cho WK *et al*. 2012 Microstructured barbs on the North American porcupine quill enable easy tissue penetration and difficult removal. *Proc. Natl Acad. Sci. USA* **109**, 21289–21294. (doi:10.1073/pnas.1216441109)
7. Crofts SB, Anderson PSL. 2018 The influence of cactus spine surface structure on puncture performance and anchoring ability is tuned for ecology. *Proc. R. Soc. B* **285**, 20182280. (doi:10.1098/rspb.2018.2280)
8. Broeckhoven C, El Adak Y, Hui C, Van Damme R, Stankowich T. 2018 On dangerous ground: the evolution of body armour in cordyline lizards. *Proc. R. Soc. B* **285**, 20180513. (doi:10.1098/rspb.2018.0513)
9. Kolmann MA, Peixoto T, Pfeiffenberger JA, Summers AP, Donatelli CM. 2020 Swimming and defence: competing needs across ontogeny in armoured fishes (Agonidae). *J. R. Soc. Interface* **17**, 20200301. (doi:10.1098/rsif.2020.0301)
10. Crofts SB, Summers AP. 2014 How to best smash a snail: the effect of tooth shape on crushing load. *J. R. Soc. Interface* **11**, 20131053. (doi:10.1098/rsif.2013.1053)
11. Freeman PW, Lemen CA. 2007 The trade-off between tooth strength and tooth penetration: predicting optimal shape of canine teeth. *J. Zool*. **273**, 273–280. (doi:10.1111/j.1469-7998.2007.00325.x)
12. Zhao ZL, Zhao HP, Ma GJ, Wu CW, Yang K, Feng XQ. 2015 Structures, properties, and functions of the stings of honey bees and paper wasps: a comparative study. *Biol. Open*. **4**, 921–928. (doi:10.1242/bio.012195)
13. Higham TE, Russell AP, Zani PA. 2013 Integrative biology of tail autotomy in lizards. *Physiol. Biochem. Zool*. **86**, 603–610. (doi:10.1086/673875)
14. Lovejoy NR. 1996 Systematics of myliobatoid elasmobranchs: with emphasis on the phylogeny and historical biogeography of neotropical freshwater stingrays (Potamotrygonidae: Rajiformes). *Zool. J. Linn. Soc*. **117**, 207–257. (doi:10.1111/j.1096-3642.1996.tb02189.x)
15. Carrier JC, Musick JA, Heithaus MR (eds). 2012 *Biology of sharks and their relatives*, 2nd edn. Boca Raton, FL: CRC Press.

16. Johansson PK, Douglass TG, Christopher GL. 2004 Caudal spine replacement and histogenesis in the round stingray. *Urobatis Halleri. Bull. South. Calif. Acad. Sci* **103**, 115–125. (doi:%2010.3160/0038-3872-103.3.115)
17. Gudger EW. 1914 History of the spotted eagle ray, *Aetobatus narinari*, together with a study of its external structures. *Pap Tortugas Lab. Carnegie Inst. Wash*. **11**, 248–323.
18. Schwartz FJ. 2007 A survey of tail spine characteristics of stingrays frequenting African, Arabian to Chagos-Maldive Archipelago waters. *Smithiana Bull*. **8**, 41–52.
19. Schwartz FJ. 2007 Tail spine characteristics of stingrays (Order Myliobatiformes) frequenting the FAO fishing area 61 (20°N 120°E–50°N 150°E) of the northwest Pacific Ocean. *Raffles Bull. Zool*. **Suppl. 14**, 121–130.
20. Schwartz FJ. 2008 A survey of the tail spine characteristics of stingrays frequenting Indo-Pacific ocean areas between the International Date Line and the Chagos Archipelago-Maldive Islands. *J. N. C. Acad. Sci.* **124**, 27–45.
21. Schwartz FJ. 2008 A survey of tail spine characteristics of stingray species (Order Myliobatiformes) frequenting the eastern Pacific Ocean from the International Dateline to the Americas. *J. N. C. Acad. Sci*. **124**, 72–81.
22. Thorson TB, Langhammer JK, Oetinger MI. 1988 Periodic shedding and replacement of venomous caudal spines, with special reference to South American freshwater stingrays, *Potamotrygon* spp. *Environ. Biol. Fish*. **23**, 299–314. (doi:10.1007/BF00005241)
23. Hughes R, Pedersen K, Huskey S. 2018 The kinematics of envenomation by the yellow stingray, *Urobatis jamaicensis*. *Zoomorphology* **137**, 409–418. (doi:10.1007/s00435-018-0404-0)
24. Diaz JH. 2008 The evaluation, management, and prevention of stingray injuries in travelers. *J. Travel Med*. **15**, 102–109. (doi:10.1111/j.1708-8305.2007.00177.x)
25. Shea-Vantine CS, Galloway KA, Ingle DN, Porter ME, Kajiura SM. 2021 Caudal spine morphology and puncture performance of two coastal stingrays. *Integr. Comp. Biol*. **61**, 749–758. (doi:10.1093/icb/icab077)
26. Dean MN, Bizzarro JJ, Clark B, Underwood CJ, Johanson Z. 2017 Large batoid fishes frequently consume stingrays despite skeletal damage. *R. Soc. Open Sci*. **4**, 170674. (doi:10.1098/rsos.170674)
27. Huskey S. 2020 Stingray spines embedded in the skull of a cobia. *Ichthyol. Res*. **68**, 214–216. (doi:10.1007/s10228-020-00767-1)
28. McFee W, Root H, Friedman R, Zolman E. 1997 A stingray spine in the scapula of a bottlenose dolphin. *J. Wildl. Dis*. **33**, 921–924. (doi:10.7589/0090-3558-33.4.921)
29. Duignan PJ, Hunter JEB, Visser IN, Jones GW, Nutman A. 2000 Stingray spines: a potential cause of killer whale mortality in New Zealand. *Aquat. Mamm.* **26**, 143–147.
30. Heithaus MR, Vaudo JJ. 2012 Predator-prey interactions. In *Biology of sharks and their relatives* (eds JC Carrier, JA Musick, MR Heithaus), pp. 505–534, 2nd edn. Boca Raton, FL: CRC Press.
31. Castello L, McGrath DG, Hess LL, Coe MT, Lefebvre PA, Petry P, Macedo MN, Renó VF, Arantes CC. 2013 The vulnerability of Amazon freshwater ecosystems. *Conserv. Lett*. **6**, 217–229. (doi:10.1111/conl.12008)
32. Fricke R, Eschmeyer WN, Fong JD. 2026 *Catalog of fishes: species by family/subfamily*. California Academy of Sciences. See https://researcharchive.calacademy.org/research/ichthyology/catalog (accessed February 2026).
33. Last PR, White WT, Carvalho MR, Séret B, Stehmann MFW (eds). 2016 *Rays of the world*. Clayton South, Australia: CSIRO Publishing.
34. Fedorov A *et al*. 2012 3D slicer as an image computing platform for the quantitative imaging network. *Magn. Reson. Imaging* **30**, 1323–1341. (doi:10.1016/j.mri.2012.05.001)
35. Rolfe S *et al*. 2021 SlicerMorph: an open and extensible platform to retrieve, visualize and analyse 3D morphology. *Methods Ecol. Evol*. **12**, 1816–1825. (doi:10.1111/2041-210x.13669)
36. Stein RW, Mull CG, Kuhn TS, Aschliman NC, Davidson LNK, Joy JB, Smith GJ, Dulvy NK, Mooers AO. 2018 Global priorities for conserving the evolutionary history of sharks, rays and chimaeras. *Nat. Ecol. Evol*. **2**, 288–298. (doi:10.1038/s41559-017-0448-4)
37. Schneider CA, Rasband WS, Eliceiri KW. 2012 NIH image to ImageJ: 25 years of image analysis. *Nat. Methods* **9**, 671–675. (doi:10.1038/nmeth.2089)
38. Crofts SB, Lai Y, Hu Y, Anderson PSL. 2019 How do morphological sharpness measures relate to puncture performance in viperid snake fangs? *Biol. Lett*. **15**, 20180905. (doi:10.1098/rsbl.2018.0905)
39. Anderson PSL. 2018 Making a point: shared mechanics underlying the diversity of biological puncture. *J. Exp. Biol*. **221**, jeb187294. (doi:10.1242/jeb.187294)
40. Evans AR, Sanson GD. 1998 The effect of tooth shape on the breakdown of insects. *J. Zool*. **246**, 391–400. (doi:10.1111/j.1469-7998.1998.tb00171.x)
41. Huie JM, Summers AP, Kawano SM. 2022 SegmentGeometry: a tool for measuring second moment of area in 3D slicer. *Integr. Org. Biol*. **4**, obac009. (doi:10.1093/iob/obac009)
42. Drummond AJ, Rambaut A. 2007 BEAST: Bayesian evolutionary analysis by sampling trees. *BMC Evol. Biol*. **7**, 214. (doi:10.1186/1471-2148-7-214)
43. R Core Team. 2024 R: a language and environment for statistical computing. Vienna, Austria: R Foundation for Statistical Computing. See https://www.r-project.org/ (accessed May 2026).
44. Baken EK, Collyer ML, Kaliontzopoulou A, Adams DC. 2021 Geomorph v4.0 and gmShiny: enhanced analytics and a new graphical interface for a comprehensive morphometric experience. *Methods Ecol. Evol*. **12**, 2355–2363. (doi:10.1111/2041-210x.13723)
45. Adams D, Collyer M, Kaliontzopoulou A, Baken E. 2026 Geomorph: software for geometric morphometric analyses. R package version 4.1.0. See https://cran.r-project.org/package=geomorph (accessed May 2026).
46. Revell LJ. 2024 Phytools 2.0: an updated R ecosystem for phylogenetic comparative methods (and other things). *PeerJ* **12**, e16505. (doi:10.7717/peerj.16505)
47. Maas SA, Ellis BJ, Ateshian GA, Weiss JA. 2012 FEBio: finite elements for biomechanics. *J. Biomech. Eng*. **134**, 011005. (doi:10.1115/1.4005694)
48. Dumont ER, Grosse IR, Slater GJ. 2009 Requirements for comparing the performance of finite element models of biological structures. *J. Theor. Biol*. **256**, 96–103. (doi:10.1016/j.jtbi.2008.08.017)
49. Marcé-Nogué J, De Esteban-Trivigno S, Escrig C, Gil L. 2016 Accounting for differences in element size and homogeneity when comparing finite element models: armadillos as a case study. *Palaeontol. Electron*. **19**, 1–22. (doi:10.26879/609)
50. Pinheiro J, Bates D, R Core Team. 2026 nlme: linear and nonlinear mixed effects models. R package version 3.1-169. See https://CRAN.R-project.org/package=nlme (accessed May 2026).
51. Ives AR. 2019 R^2s for correlated data: phylogenetic models, LMMs, and GLMMs. *Syst. Biol*. **68**, 234–251. (doi:10.1093/sysbio/syy060)
52. Abburi R, Praveena M, Priyakanth R. 2021 TinkerCad - a web based application for virtual labs to help learners think, create and make. *J. Eng. Educ. Transform*. **34**, 535. (doi:10.16920/jeet/2021/v34i0/157209)
53. Anderson PSL, Kawano SM. 2022 Different traits at different rates: the effects of dynamic strain rate on structural traits in biology. *Integr. Comp. Biol*. **62**, 683–699. (doi:10.1093/icb/icac066)
54. Tonna R, Chatzistergos PE, Wyatt O, Chockalingam N. 2024 Reliability and validity of shore hardness in plantar soft tissue biomechanics. *Sensors* **24**, 539. (doi:10.3390/s24020539)
55. Hodge JR, Alim C, Bertrand NG, Lee W, Price SA, Tran B, Wainwright PC. 2018 Ecology shapes the evolutionary trade-off between predator avoidance and defence in coral reef butterflyfishes. *Ecol. Lett*. **21**, 1033–1042. (doi:10.1111/ele.12969)

56. Stankowich T, Stensrud C. 2019 Small but spiny: the evolution of antipredator defenses in Madagascar tenrecs. *J. Mammal*. **100**, 13–20. (doi:10.1093/jmammal/gyz003)
57. Strathmann RR. 1981 The role of spines in preventing structural damage to echinoid tests. *Paleobiology* **7**, 400–406. (doi:10.1017/s0094837300004693)
58. Gudger EW. 1932 Cannibalism among the sharks and rays. *Sci. Mon.* **34**, 403–419.
59. Tsafnat N, Fitz Gerald JD, Le HN, Stachurski ZH. 2012 Micromechanics of Sea Urchin spines. *PLoS One* **7**, e44140. (doi:10.1371/journal.pone.0044140)
60. Harris RJ, Jenner RA. 2019 Evolutionary ecology of fish venom: adaptations and consequences of evolving a venom system. *Toxins* **11**, 60. (doi:10.3390/toxins11020060)
61. Rennolds CW, Bely AE. 2023 Integrative biology of injury in animals. *Biol. Rev*. **98**, 34–62. (doi:10.1111/brv.12894)
62. Galloway KA, Porter ME. 2019 Mechanical properties of the venomous spines of *Pterois volitans* and morphology among lionfish species. *J. Exp. Biol*. **222**, jeb197905. (doi:10.1242/jeb.197905)
63. Bosher BT, Newton SH, Fine ML. 2006 The spines of the channel Catfish *Ictalurus punctatus* as an anti-predator adaptation: an experimental study. *Ethology* **112**, 188–195. (doi:10.1111/j.1439-0310.2006.01146.x)
64. Bronstein O, Kroh A. 2018 Needle in a haystack—genetic evidence confirms the expansion of the alien echinoid *Diadema setosum* (Echinoidea: Diadematidae) to the Mediterranean coast of Israel. *Zootaxa* **4497**, 593–599. (doi:10.11646/zootaxa.4497.4.9)
65. Stock SR, Ebert TA, Ignatiev K, De Carlo F. 2006 Structures, structural hierarchy, and function in Sea Urchin spines. In *Developments in X-ray tomography V* (ed. U Bonse), p. 63180A, vol. **6318**. San Diego, CA: SPIE. (doi:10.1117/12.679548)
66. Vincent JFV, Owers P. 1986 Mechanical design of hedgehog spines and porcupine quills. *J. Zool*. **210**, 55–75. (doi:10.1111/j.1469-7998.1986.tb03620.x)
67. Pedroso CM, Jared C, Charvet-Almeida P, Almeida MP, Garrone Neto D, Lira MS, Haddad V Jr, Barbaro KC, Antoniazzi MM. 2007 Morphological characterization of the venom secretory epidermal cells in the stinger of marine and freshwater stingrays. *Toxicon* **50**, 688–697. (doi:10.1016/j.toxicon.2007.06.004)
68. Barbaro KC, Lira MS, Malta MB, Soares SL, Garrone Neto D, Cardoso JLC, Santoro ML, Haddad Junior V. 2007 Comparative study on extracts from the tissue covering the stingers of freshwater (*Potamotrygon falkneri*) and marine (*Dasyatis guttata*) stingrays. *Toxicon* **50**, 676–687. (doi:10.1016/j.toxicon.2007.06.002)
69. Crofts SB, Anderson PSL. 2023 How venom pore placement may influence puncture performance in snake fangs. *J. Exp. Biol*. **226**, jeb245666. (doi:10.1242/jeb.245666)
70. Loke LHL, Chisholm RA. 2022 Measuring habitat complexity and spatial heterogeneity in ecology. *Ecol. Lett*. **25**, 2269–2288. (doi:10.1111/ele.14084)
71. Kirchhoff KN, Klingelhöfer I, Dahse HM, Morlock G, Wilke T. 2014 Maturity-related changes in venom toxicity of the freshwater stingray *Potamotrygon leopoldi*. *Toxicon* **92**, 97–101. (doi:10.1016/j.toxicon.2014.10.011)
72. Vaudo JJ, Heithaus MR. 2012 Diel and seasonal variation in the use of a nearshore sandflat by a ray community in a near pristine system. *Mar. Freshw. Res*. **63**, 1077–1084. (doi:10.1071/mf11226)
73. Martins APB, Heupel MR, Bierwagen SL, Chin A, Simpfendorfer C. 2020 Diurnal activity patterns and habitat use of juvenile *Pastinachus ater* in a coral reef flat environment. *PLoS One* **15**, e0228280. (doi:10.1371/journal.pone.0228280)
74. Poisson F, Ellis JR, McCully Phillips SR. 2024 Preliminary insights on the habitat use and vertical movements of the pelagic stingray (*Pteroplatytrygon violacea*) in the western Mediterranean Sea. *Fishes* **9**, 238. (doi:10.3390/fishes9060238)
75. Strong WR, Snelson FF, Gruber SH. 1990 Hammerhead shark predation on stingrays: an observation of prey handling by *Sphyrna mokarran*. *Copeia* **1990**, 836–840. (doi:10.2307/1446449)
76. Nifong JC, Lowers RH. 2017 Reciprocal intraguild predation between *Alligator mississippiensis* (American alligator) and Elasmobranchii in the southeastern United States. *Southeast. Nat*. **16**, 383–396. (doi:10.1656/058.016.0306)
77. Ajemian MJ, Dolan D, Graham WM, Powers SP. 2011 First evidence of elasmobranch predation by a waterbird: stingray attack and consumption by the great blue heron (*Ardea herodias*). *Waterbirds* **34**, 117–120. (doi:10.1675/063.034.0116)
78. Best RC, da Silva VMF. 1993 *Inia geoffrensis*. *Mamm. Species* **426**, 1–8. (doi:10.2307/3504090)
79. Prestes de Souza L. 2020 Pesca dos grandes bagres migradores na bacia Amazônica: uma trajetória de sobrepesca. PhD dissertation, [Brazil]: Universidade Federal do Pará. https://www.ppgeap.propesp.ufpa.br/ARQUIVOS/teses/2020/Luiza%20Prestes.pdf.
80. Lucifora LO, Bellagamba PJ, Vega LE, Bó MS, Alvarenga PF, Astarloa JM. 2020 Significance of stingrays (Chondrichthyes: Myliobatiformes) as prey of crocodilians (Reptilia: Crocodylia) in non-marine environments. *Ichthyol. Explor. Freshwat.* **30**, 179–192. (doi:10.23788/IEF-1122)
81. Galloway KA, Porter ME. 2021 Predator-prey interactions examined using lionfish spine puncture performance. *Integr. Org. Biol*. **3**, obaa049. (doi:10.1093/iob/obaa049)
82. Stankowich T, Campbell LA. 2016 Living in the danger zone: exposure to predators and the evolution of spines and body armor in mammals. *Evolution* **70**, 1501–1511. (doi:10.1111/evo.12961)
83. Magnuson A, Dean MN, Weaver JC, Fontenelle JP, Lovejoy NR, Kolmann MA. 2024 Independent transitions to freshwater environments promote phenotypic divergence, not convergence, in stingrays. *Integr. Comp. Biol*. **64**, 1437–1453. (doi:10.1093/icb/icae023)
84. Enzor LA, Wilborn RE, Bennett WA. 2011 Toxicity and metabolic costs of the Atlantic stingray (*Dasyatis sabina*) venom delivery system in relation to its role in life history. *J. Exp. Mar. Biol. Ecol*. **409**, 235–239. (doi:10.1016/j.jembe.2011.08.026)
85. Poulin E, Kolmann MA, Stiassny MLJ, Cohen KE, Huie JM, Chabain J, Martinez CM. 2026 Stingray spine diversity reflects performance trade-offs linked to puncture and breakability [Dataset and code]. Dryad. (doi:10.5061/dryad.7d7wm387k)
86. Poulin E, Kolmann MA, Stiassny MLJ, Cohen KE, Huie JM, Chabain J, Martinez CM. 2026 Stingray spine diversity reflects performance trade-offs linked to puncture and breakability. Figshare. (doi:10.6084/m9.figshare.32358438)
87. Poulin E *et al*. 2026 Supplementary material from: Stingray spine diversity reflects performance trade-offs linked to puncture and breakability. Figshare. (doi:10.6084/m9.figshare.c.8533457)